Organic Electronics 9 (2008) 821–828

Contents lists available at ScienceDirect

Organic Electronics

journal homepage: www.elsevier.com/locate/orgel

Controlled nanorubbing of polythiophene thin films for field-effect transistors

G. Derue [a,b,*], D.A. Serban [c], Ph. Leclère [a], S. Melinte [c], P. Damman [b], R. Lazzaroni [a]

[a] Laboratory for Chemistry of Novel Materials, Center for Innovation and Research in Materials and Polymers – CIRMAP, University of Mons-Hainaut, Place du Parc 20, B-7000 Mons, Belgium

[b] Laboratoire Interfaces and Fluides Complexes, Center for Innovation and Research in Materials and Polymers – CIRMAP, University of Mons-Hainaut, Place du Parc 20, B-7000 Mons, Belgium

[c] CERMIN, Université catholique de Louvain, B-1348 Louvain-la-Neuve, Belgium

ARTICLE INFO

Article history:
Received 21 March 2008
Received in revised form 27 May 2008
Accepted 28 May 2008
Available online 20 June 2008

PACS:
82.35.Cd
87.64.Dz
81.07.Nb

Keywords:
Nanorubbing
Poly(thiophene)
Field-effect transistors

ABSTRACT

We present results obtained by applying the nanorubbing process to improve the electrical performance of regioregular poly(3-hexylthiophene-2,5-diyl) (P3HT) thin films. Essentially, we use a scanning atomic force microscope tip to induce a controlled deformation on the surface consisting of parallel grooves with a period imposed by the scanning parameters. The optical characterization of the rubbed zones highlights an orientation of P3HT chains along the scanning direction. When the nanorubbing process is orienting the polymer chains within the channel of a field-effect transistor, we observe that the charge carrier mobility increases (decreases) when the tip scans parallel (perpendicular) to the source–drain axis. This difference likely stems from the polymer chains orientation induced by the alignment process.

1. Introduction

Among conjugated polymers, regioregular poly(3-hexylthiophene-2,5-diyl) (P3HT), which combines high field-effect mobility (up to 0.18 cm^2/Vs) [1] and good solution-processability, is stimulating much interest as active electronic element in various thin film devices. Since the charge transport properties are intimately related to the long-range order [2], it is therefore essential to enhance the degree of structural order in conjugated polymer thin films for improved device performance. Conjugated polymer films have complex microstructures, where uncorrelated microcrystalline domains are embedded in an amorphous matrix limiting the charge mobility [3]; the presence of disorder implies that charge transport is best described by hopping models [4]. Strong π–π intermolecular interactions, combined to the crystallization of the alkyl side groups, induce better structural order, which leads to optimal charge transport. In this context, it is of prime importance to control the crystallinity, the chain orientation and the morphology of the polymer layer.

Various methods can be used to impart order to conjugated polymer films: stretching [5], Langmuir–Blodgett deposition [6] or the "friction-transfer" technique [7]. Recently, we have shown that rubbing thin polythiophene films with a velvet cloth leads to the orientation of the chains at the polymer surface parallel to the rubbing direction [8]. Interestingly, this type of surface modification can also be achieved at microscopic lengthscales, with precise control of the size and the localization of the rubbed areas,

* Corresponding author. Address: Laboratory for Chemistry of Novel Materials, Center for Innovation and Research in Materials and Polymers – CIRMAP, University of Mons-Hainaut, Place du Parc 20, B-7000 Mons, Belgium. Tel.: +32 65 37 38 65; fax: +32 65 37 38 61.
E-mail address: derueg@averell.umh.ac.be (G. Derue).

1566-1199/$ - see front matter © 2008 Elsevier B.V. All rights reserved.
doi:10.1016/j.orgel.2008.05.024

by using a small-size rubbing device. The nanorubbing process, which consists in the deformation of a polymer thin film by scanning an Atomic Force Microscopy (AFM) tip operating in contact mode, has been first used to align polyimide layers. The structural anisotropy resulting from nanorubbing was demonstrated to be sufficiently strong to induce efficient liquid crystal orientation even at a moderate load force [9,10].

In this paper, we report on the application of the nanorubbing technique to P3HT thin films. Our aim is to study the effect of chain orientation on the field-effect transistor (FET) properties by nanorubbing P3HT thin deposits that constitute the active layer in the FET channel. It has been shown previously that charge transport in polymer FETs is highly dependent on the orientation of the crystalline domains relative to the carrier transport direction (from source to drain) [11]. We critically test the nanorubbing technique and find that, indeed, FETs display different properties, depending on the orientation of the alignment process [12].

2. Experimental section

2.1. Thin film preparation

RR–P3HT with a regioregularity of 99.8% was obtained from Aldrich. P3HT thin films were prepared by dip-coating clean silicon substrates into chloroform solutions (5 mg/ml) of RR–P3HT; the substrate is immersed one time and stays 30 s in the polymer solution; the retracting speed is 70 mm/min. Typical film thicknesses are in the 5–10 nm range, as determined by ellipsometry and AFM. The FETs are designed in the bottom-gate bottom-contact configuration. The devices were fabricated from a doped silicon substrate, which plays the role of the gate supporting a 100 nm thick SiO_2 dielectric. The SiO_2 layer capacitance C_i was measured to be 33 nF/cm^2. The source and drain electrodes were deposited by electron-beam evaporation of 70 nm Pd with a 1 nm thick Ti adhesion layer. Typical channel width (W) dimensions are 25- and 100-μm with corresponding channel length (L) sizes of 1- and 30-μm. The P3HT active layers were formed by dipping those structures in chloroform solutions, following the above described protocol.

2.2. Nanorubbing

The nanorubbing process was performed with a Nanoscope IIIa AFM microscope working in contact mode. The tips are made of antimony-doped silicon with a spring constant of 2 ± 0.5 N/m. [13] Typically 10 consecutive rubbing scans were carried out with the AFM tip in order to induce a sufficient deformation on the P3HT deposits. The loading force applied by the tip on the film during nanorubbing is approximately 200 nN, as calculated from the approach–retract curves.

2.3. AFM imaging

The AFM imaging was performed in "Tapping-mode" (TMAFM). In this mode, the cantilever holding the probe tip oscillates close to the resonance frequency (ca. 300 kHz) above the sample surface so that the tip is in intermittent contact with the surface at the lower end of the oscillation. Since no lateral force is applied by the tip on the surface during TMAFM operation, no further surface modification is expected to occur in those conditions. The phase of the oscillating tip is very sensitive to the nature of the interaction with the surface. It has been shown that the phase lag is related to the mechanical response of the material when the amplitude is only slightly damped upon contact with the surface. [14–16] Therefore, simultaneous acquisition of the phase and the height image provides a map of the local mechanical response. The AFM images were recorded with a Nanoscope IIIa microscope operated at room temperature in air using commercial cantilevers made of antimony-doped silicon with a spring constant of 30 N/m. The images were digitally sampled at the maximum number of pixels (512) in each direction, and the Nanoscope image processing software was used for image analysis. Unless otherwise stated, image treatment was limited to a "flattening" operation, whereby a first-order surface representing height variations related to a possible tilt of the sample is subtracted from the original image.

2.4. FET characterization

The drain current I_d vs. drain bias V_d (output) and I_d vs. gate bias V_g (transfer) characteristics have been collected in ambient conditions with an Agilent 4156C Precision Semiconductor Parameter Analyzer.

3. Results and discussion

In a typical experiment, we have unidirectionally rubbed, with the AFM tip in contact mode, a $(10 \times 10)\ \mu m^2$ area on a P3HT film prepared by dip-coating. Afterwards, the morphology of the rubbed regions was investigated by TMAFM. Fig. 1a shows height and phase images in an area across the modified region. The rubbed area is barely visible in the height image (left) and appears more clearly in the phase image (right). This phase contrast originates from local differences in tip-sample interactions, which indicates that the nanorubbing process induces a modification in the polymer mechanical response. Since rubbing favors polymer crystallization via chain alignment [17] and we observe a clear optical signature of P3HT chain alignment in the rubbed areas (see below), it is most likely the change in TMAFM phase signal over the rubbed areas is due a local increase in stiffness, as a result of P3HT chain ordering.

Upon closer inspection, we observe that the rubbed area presents, both in the height and phase images, a regular pattern made of grooves parallel to the rubbing direction (Fig. 1b). From the Fourier transform of the height image (see inset), the period of the pattern is found to be about 40 nm. This value is directly related to the experimental conditions of the rubbing process. The $(10 \times 10)\ \mu m^2$ area was scanned by 256 parallel lines and the lateral shift between two lines is therefore (10,000 (nm)/256 = 39 (nm)), which corresponds to the period of the pattern formed in

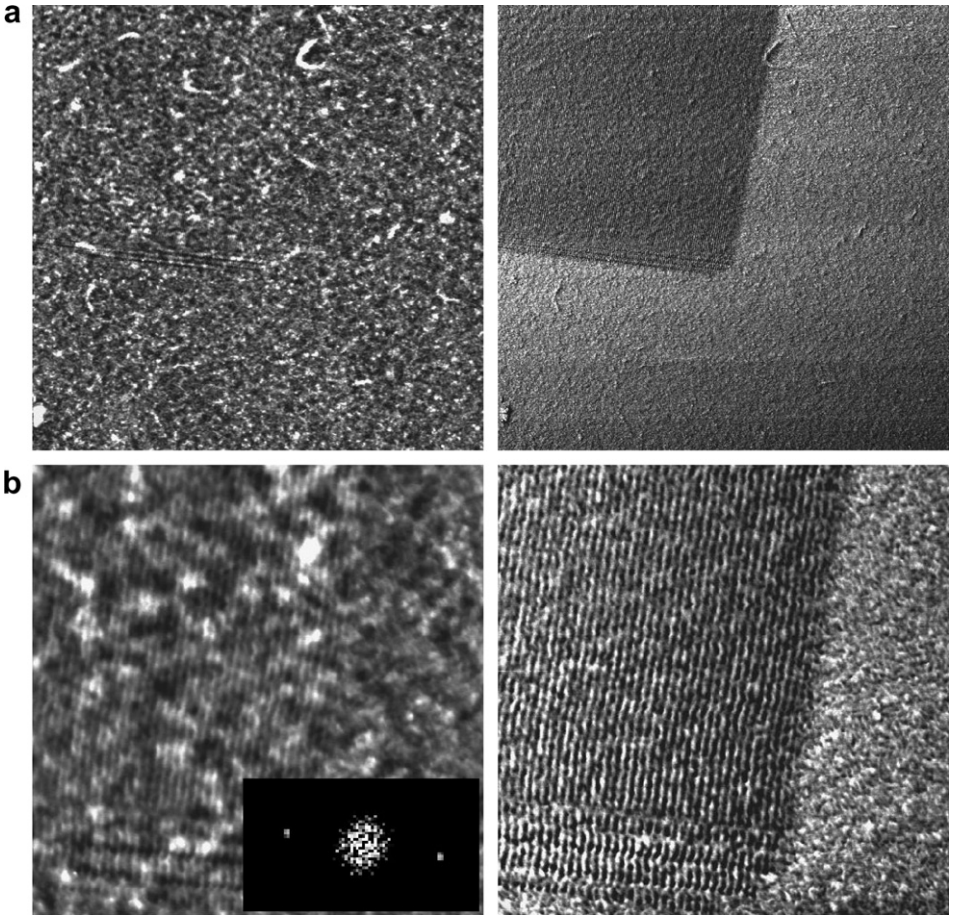

Fig. 1. (a) $(10 \times 10)\ \mu m^2$ and (b) $(2.5 \times 2.5)\ \mu m^2$ TMAFM height (left) and phase (right) images of a nanorubbed area. The vertical gray scale is 10 nm and 20° for the height and phase image, respectively. Inset: Fourier transform of the height image.

the rubbed zone. Under the conditions used here (10 rubbing scans with a load of 200 nN), the vertical amplitude of the pattern is 1.5 ± 0.5 nm.

Based on these observations, it therefore becomes possible to generate patterns with a well-defined periodicity, by selecting the size of the rubbed area and the resolution of the scanning during the rubbing operation. Two examples are shown in Fig. 2. In image Fig. 2a, a square of $(5 \times 5)\ \mu m^2$ was rubbed with a resolution of 32 lines/scan. Accordingly, the grooves period is around 150 nm (5000 (nm)/32 = 156 (nm)). A closer look reveals that the lines are not perfectly parallel, but correspond to a very tight zig–zag pattern. This is even clearer upon further reducing the resolution to 16 lines/scan (Fig. 2b). This reflects the actual tip displacement during the rubbing: the tip scans back and forth in the fast scan direction while slowly moving in the orthogonal direction (Fig. 2c), giving rise to the zig–zag pattern. Nevertheless, for more realistic rubbing conditions (256 lines/scan) used for FET characterization, the lines can be considered to be parallel.

In order to highlight a possible orientation of the polymer chains within the rubbed zone, the samples were analyzed with optical microscopy between crossed polars. As an example, two P3HT films with four $(10 \times 10)\ \mu m^2$ rubbed square areas are shown in Fig. 3; all the nanorubbed domains appear with a high birefringence. In addition, complete extinction of these squares is observed when the polars are oriented either parallel or perpendicular to the rubbing direction. These observations clearly testify the orientation of the polymer chains induced by the rubbing process.

When using a single polar, we observe that the rubbed areas appear darker when it is oriented parallel to the rubbing direction while they are brighter when the orientation is perpendicular to the rubbing direction. This difference in the light absorption indicates that the chains are oriented along the rubbing direction, since it is well known that the first optical transition in conjugated polymers is polarized along the chain axis [18]. The polymer chains orientation is most probably due to the combination of the shear stress induced by the tip displacement and the ability of the regioregular polymer to crystallize.

Since regioregular P3HT is partly crystalline [19], we propose that the anisotropy appearing upon rubbing is due to the alignment of preexisting crystalline domains and/or to the stretching and crystallization of chains in

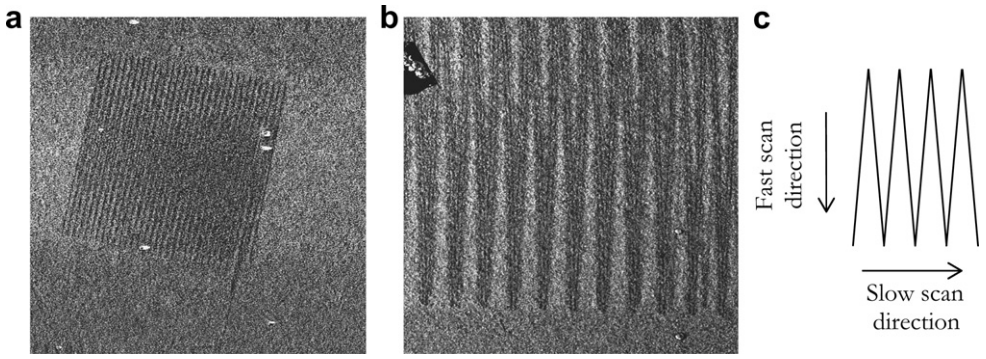

Fig. 2. (a) (10×10) μm^2 TMAFM phase image of a nanorubbed P3HT film with a resolution of 32 lines/scan. The vertical gray scale is 30°. (b) (4×4) μm^2 TMAFM phase image of a nanorubbed P3HT film with a resolution of 16 lines/scan. The vertical gray scale is 15°. (c) Scheme of the tip scan pattern. The dark regions in images (a) and (b) correspond to the zones where the tip has rubbed the film surface.

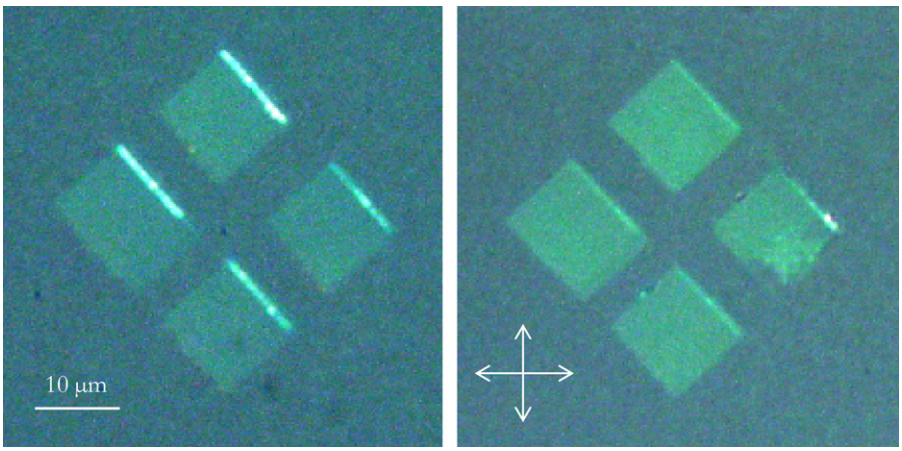

Fig. 3. Optical micrographs between crossed polars for P3HT films with four (10×10) μm^2 rubbed squares. The crossed polars are oriented as shown by the white arrows.

the amorphous regions. In a control experiment, nanorubbing has been carried out on thin films of regiorandom P3HT, which cannot crystallize due to the random arrangement of the hexyl side groups. In that case, neither changes in the surface morphology nor birefringence are observed, which is consistent with the absence of polymer chain orientation. In the regiorandom system, the polymer chains that are stretched by the tip displacement most probably relax back to the coiled state very quickly afterwards.

In order to study the effect of chain orientation on the device electrical properties, we applied the nanorubbing technique to P3HT thin films defining the channel of FETs. The rubbed area includes the P3HT channel and a part of the electrodes, because the polymer layer, deposited by dip-coating, covers the devices entirely. The TMAFM height image (top left) in Fig. 4a shows the P3HT channel as the dark horizontal region comprised between the source and drain electrodes, which appear in gray. The corresponding phase image (top right) shows no contrast between the channel and the electrodes, consistent with the fact that the whole device surface is covered with P3HT. The pattern generated by the rubbing is clearly observed in the close-ups (Fig. 4b); it is very similar to that obtained on the 'free' P3HT films.

Fig. 5 displays optical micrographs of a P3HT FET with a nanorubbed zone across the channel. Rubbing has been performed over a (25×25) μm^2 area, with the scan direction along the electrodes, as indicated by the arrow in the right micrograph. Between crossed polars, the electrodes appear in pale blue and the rubbed area is very bright (yellow over SiO_2 and blue over Pd source and drain electrodes) when the rubbing direction is at 45° with respect to the polars (left image), which indicates that also in this system the rubbed polymer is birefringent. Consistently, a complete extinction of the rubbed square is observed when the rubbing direction is either parallel or perpendicular to the polarization directions, testifying to the polymer chain orientation within the rubbed domain and so within the P3HT channel.

4. FETs properties

The typical output (a) and transfer (b) characteristics of P3HT FETs fabricated with $W = 25$ μm, $L = 1$ μm and

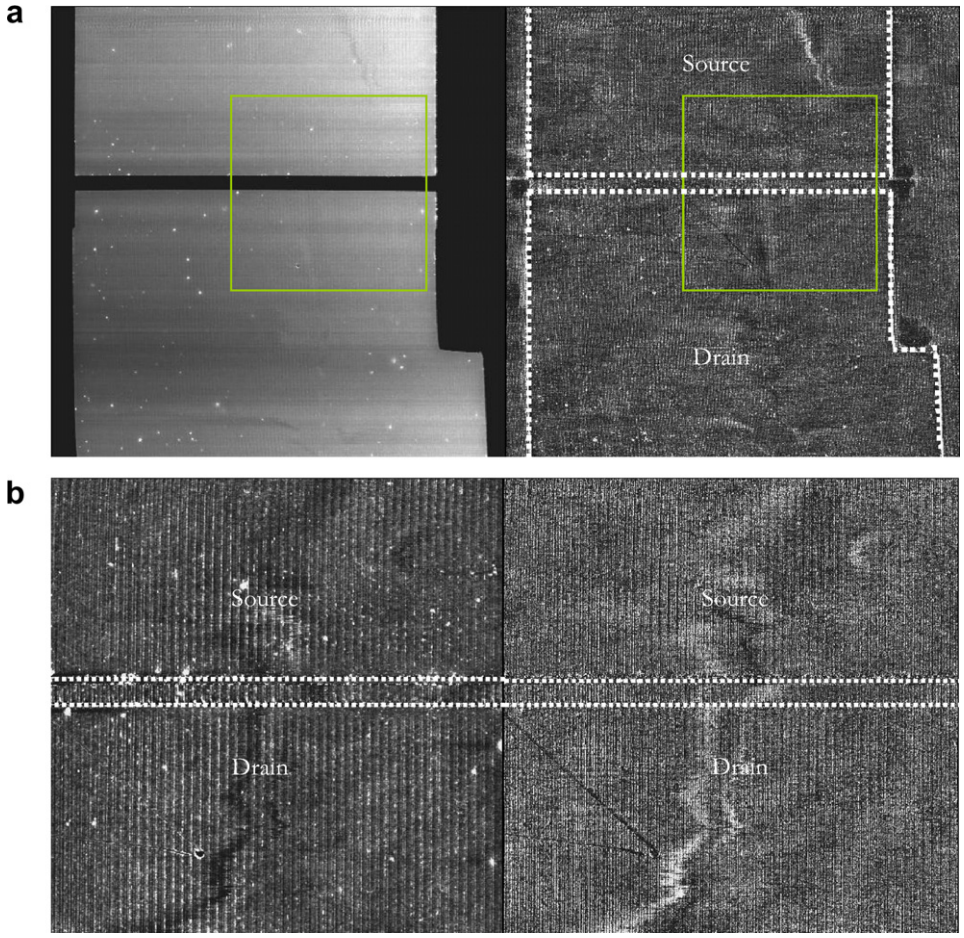

Fig. 4. (a) $(35 \times 35)\,\mu m^2$ and (b) $(15 \times 15)\,\mu m^2$ TMAFM height (left) and phase (right) images of a channel-rubbed field-effect transistor. Images (b) correspond to green squared areas in images (a). The vertical gray scale is 7 nm for height images and 25° for phase images.

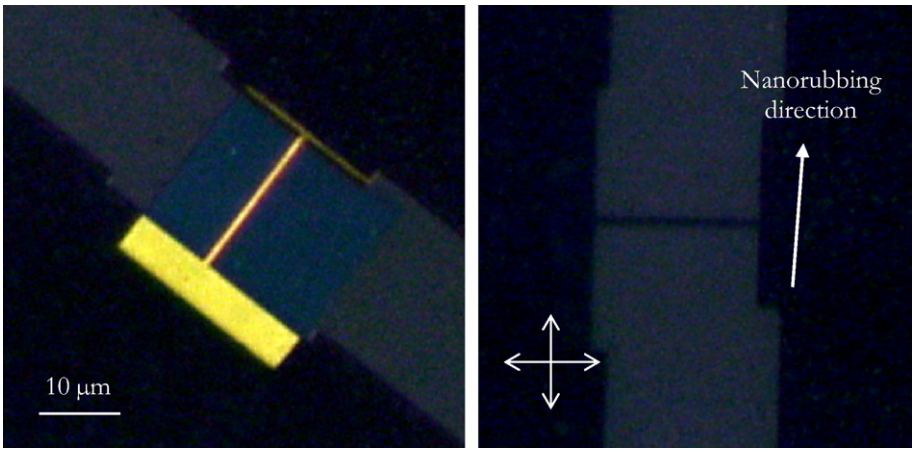

Fig. 5. Optical micrographs between crossed polars of a P3HT field-effect transistor with the channel structured by nanorubbing. The crossed polars are oriented as shown by the white arrows.

pristine SiO_2 dielectrics [20,21] are given in Fig. 6. These transistors display short channel effects [22,23], in other words inability of the drain current to saturate above the pinch-off. We have consequently determined the field-effect mobility at both low and high drain voltages, as shown hereafter. The on/off current ratio of our FETs is

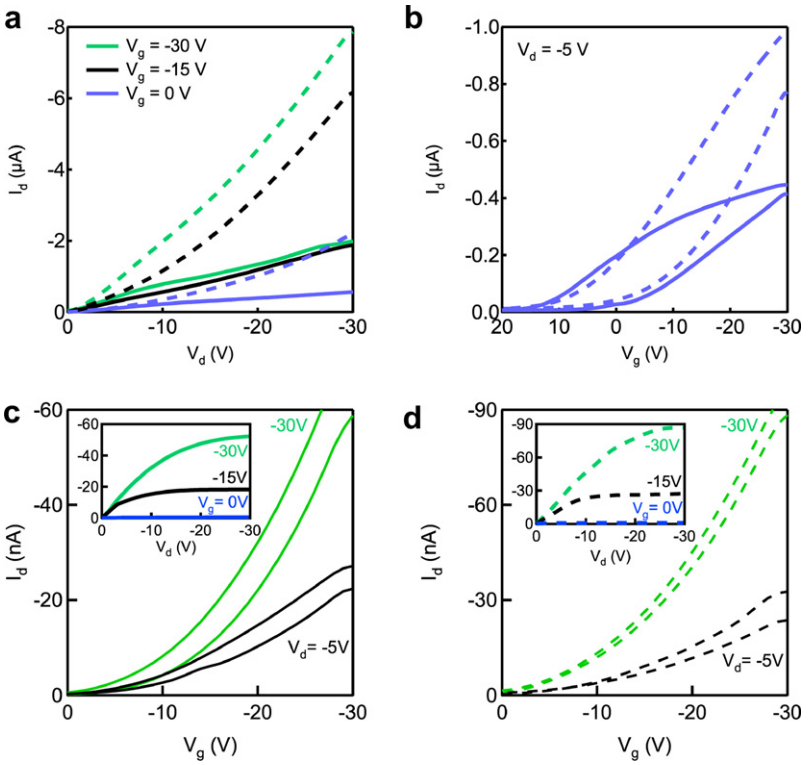

Fig. 6. Output (a) and transfer (b) characteristics of P3HT FETs with $W = 25$ μm, $L = 1$ μm and pristine SiO_2 dielectrics. (c) and (d) Transfer behavior of P3HT FETs with $W = 100$ μm, $L = 30$ μm and hexamethyldisilazane-treated SiO_2 dielectrics. Insets display their respective output response. Before rubbing (continuous curves) and after rubbing (dashed curves).

below 1000, similar to previous reports, which affirmed unintentional doping of the P3HT when processed in ambient conditions [24,25]. This unfortunately precludes the extraction of certain parameters, such as maximum transconductance and cut-off frequency, i.e., a more in-depth analysis of the electrical changes induced by the nanorubbing process. Note that the transfer characteristics (Fig. 6b) show a pronounced hysteresis, typical of thick SiO_2 dielectrics, which indicates a relatively high density of traps at the organic/dielectric interface and within the dielectric [26]. As proper treatment of the dielectric reduces the hysteresis, we have also tested devices with $W = 100$ μm, $L = 30$ μm, and hexamethyldisilazane-coated 100-nm-thick SiO_2 dielectrics. Their corresponding current–voltage characteristics are given in panels (c) and (d) of Fig. 6. Indeed, they display lower hysteresis with respect to pristine SiO_2 devices together with a well-defined saturation of the $I_d - V_d$ curves (see insets).

To quantify the impact of nanorubbing process on the FET characteristics, we have determined the linear mobility μ_{lin} using the equation $I_d = W/L{*}C_i{*}\mu_{lin}{*}(V_g - V_{th}){*}V_d$, where the threshold voltage V_{th} has been extracted from plots of $I_d/g_m^{1/2}$ vs. V_g. Here $g_m = \partial I_d/\partial V_g$ is the transconductance. Given the presence of superlinearities at low V_g in the output characteristics of the $L = 1$ μm FETs, the extracted values for the linear mobility might be questionable. We therefore provide the field-effect mobility also at high gate voltages, using the equation $I_d = W/2L{*}C_i{*}\mu_{sat}{*}(V_g - V_{th\ sat})^2$. The $V_{th\ sat}$ has been extracted from plots of $I_d^{1/2}$ vs. V_g. Table 1 compares all these parameters for the homogeneous and nanorubbed devices (along the electrode direction). We observe two times or higher mobilities for the nanorubbed FETs, comparable with published data for standard bottom-contact P3HT devices [27]. From the transfer plots we have also extracted the source-drain series resistance (R_{sd}), using the technique detailed by Rhayem and collaborators [28] and found values in

Table 1
Electrical properties of the homogeneous and nanorubbed P3HT FETs (along the electrode direction)

Device		V_{th} (V)	μ_{lin} (cm^2/V s)	R_{sd} (MΩ)	$V_{th\ sat}$ (V)	μ_{sat} (cm^2/V s)
$W = 25$ μm $L = 1$ μm	Homogeneous	12	2.6×10^{-3}	5	−4	7×10^{-3}
	Nanorubbing//	7	6.4×10^{-3}	1	2	20×10^{-3}
$W = 100$ μm $L = 30$ μm	Homogeneous	−6	2.0×10^{-3}	50	0	1×10^{-3}
	Nanorubbing//	−10	3.0×10^{-3}	35	0	2×10^{-3}

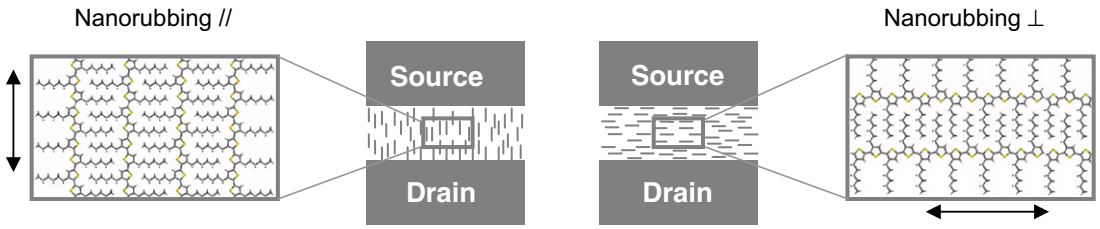

Fig. 7. Schematic representation of the P3HT chain arrangement when the nanorubbing is performed parallel (left) and perpendicular (right) to the source–drain axis. The polymer chains and the electrodes are not to scale. The double arrows indicate the rubbing direction.

the MΩ range, consistent with previous reports on P3HT films deposited by spin coating [29,30]. This indicates that the nanorubbing process provides a gentle modification of the metal/polymer charge–injection interface. Finally, we have checked that the mobility value does not depend on the direction of the dip-coating operation, i.e., either parallel or perpendicular to the electrodes. In other words, in the conditions we used, the dip-coating does not induce significant orientation of the P3HT film.

After rubbing the P3HT channel along the electrode direction (i.e., as indicated in Fig. 5), the transistors operate nicely, with improved parameters (see Table 1). In contrast, when the nanorubbing is performed perpendicular to the electrode direction, the mobility has consistently been found lower and approaching 10^{-4} cm^2/V s. This contrast in mobility is most probably related to the difference in chain orientation induced by the rubbing. It has been shown previously [8] that rubbing P3HT films leads to a global orientation of the chains at the surface, with the (100) plane perpendicular to the polymer layer. This means that the plane of individual polymer molecules is parallel to the surface. Let us note that such arrangement is not the most favorable for charge transport in the plane of the polymer film (a 'edge-on' organization has been shown to lead to the highest mobilities) [11]. When rubbing is carried out perpendicular to the source–drain axis, the chains are therefore arranged flat on the surface and perpendicular to the transport direction (Fig. 7, right). In such configuration, charge transport in the source-drain direction implies chain-to-chain hopping over a large distance (because of the presence of the alkyl groups), which is consistent with the low mobility observed. In contrast, when nanorubbing is performed parallel to the source–drain axis, the chains are oriented parallel to the transport direction (Fig. 7, left). Intramolecular transport is favoured and only a few inter-chain hopping events are necessary for charges to cross the channel. This is consistent with the twofold increase in mobility with respect to the homogeneous layer, in which the chain orientation is random. This behavior is similar to that recently observed when the chain orientation is promoted in poly(3,3‴-didodecyl-quaterthiophene) by embossing the polymer layer in the liquid-crystalline state [31]. Finally, we note that additional mechanisms could affect the mobilities of nanorubbed transistors. Precisely, the surface roughness induced to the polymer films constituting the FET channel by the rubbing process is likely to induce a nonuniformity in the electric field and, hence, a modification of their respective field-effect mobilities. This side effect cannot be ruled out and might play a role in our experiments. Yet, we believe that it should be strongly related to the magnitude of the corrugation (depth of the nanogrooves) as well as the periodicity of the surface deformation, and this has been not observed in the experiments.

5. Conclusions

We have applied the nanorubbing process, which uses an AFM tip operating in contact mode, to structure regioregular P3HT thin films. Rubbing induces a slight deformation on the surface, showing up as grooves to the fast scan direction, along with a modification of the mechanical response corresponding most probably to shear-induced orientation of crystalline domains. Polarized optical microscopy clearly indicates that the P3HT chains are oriented along the rubbing direction. Consistently, thin films of regiorandom P3HT, which cannot crystallize, show no morphological modifications and no optical anisotropy upon nanorubbing.

In order to study the effect of chain orientation on the electrical properties of P3HT devices, we applied the nanorubbing technique to structure the P3HT film deposited in the channel of FETs. When nanorubbing is carried out parallel to the source–drain axis, the electrical performances of the devices (such as the linear and saturation mobilities) are improved with respect to FETs employing isotropic P3HT films. In contrast, when nanorubbing is performed perpendicular to the source–drain direction, the mobility decreases. These effects are related to the polymer chain orientation: in the latter case, the chains are perpendicular to the transport direction and the charge transport implies chain-to-chain hopping over large distance, which leads to low mobilities. When the nanorubbing is performed parallel to the source-drain axis, the chains are parallel to the transport direction, intramolecular transport is favored, leading to higher mobilities.

Acknowledgments

This work was supported by the Belgian National Fund for Scientific Research (F.R.S. – FNRS), by the Belgian Federal Science Policy Office in the framework of the 'Pôle d'Attraction Interuniversitaire' program (PAI 6/27), and by Région Wallonne (ETIQUEL project). P. Damman, Ph. Leclère and S. Melinte are Research Associates of the F.R.S. – FNRS. G. Derue is grateful to FRIA for a doctoral fellowship.

References

[1] G.M. Wang, J. Swensen, D. Moses, A.J. Heeger, J. Appl. Phys. 93 (2003) 6137.
[2] H.G.O. Sandberg, G.L. Frey, M.N. Shkunov, M.M. Nielsen, C. Kumpf, Langmuir 18 (2002) 10176.
[3] H. Sirringhaus, P.J. Brown, R.H. Friend, M.M. Nielsen, K. Bechgaard, B.M.W. Langeveld-Voos, A.J.H. Spiering, R.A.J. Janssen, E.W. Meijer, Synth. Met. 111 (2001) 129.
[4] H. Yang, T.J. Shin, L. Yang, K. Cho, C.Y. Ryu, Z. Bao, Adv. Funct. Mater. 15 (2005) 671.
[5] J. Mardalen, E.J. Samuelsen, O.R. Gautun, P.H. Carlsen, Synth. Met. 48 (1992) 363.
[6] S.K. Sharma, R. Singhal, B.D. Malhotra, N. Sehgal, A. Kumar, Electrochim. Acta 49 (2004) 2479.
[7] S. Nagamatsu, W. Takashima, K. Kaneto, Macromolecules 36 (2003) 5252.
[8] G. Derue, S. Coppée, S. Gabriele, M. Surin, V. Geskin, F. Monteverde, Ph. Leclère, R. Lazzaroni, P. Damman, J. Am. Chem. Soc. 127 (2005) 8018.
[9] J.-H. Kim, M. Yoneya, J. Yamamoto, H. Yokoyama, Nanotechnology 13 (2002) 133.
[10] J.-H. Kim, M. Yoneya, H. Yokoyama, Nature 420 (2002) 159.
[11] H. Sirringhaus, P.J. Brown, R.H. Friend, M.M. Nielsen, K. Bechgaard, B.M.W. Langeveld-Voss, A.J.H. Spiering, R.A.J. Janssen, E.W. Meijer, P. Herwig, D.M. de Leeuw, Nature 401 (1999) 685.
[12] S. Scheinert, T. Doll, A. Scherer, G. Paasch, I. Hörselmann, Appl. Phys. Lett. 84 (2004) 4427.
[13] We have also used AFM cantilevers with higher or smaller spring constants to perform the nanorubbing process; we have observed that the cantilevers with intermediate spring constant (around 2 N/m) give the best results in terms of reproducibility and control of the applied force, with lower risk of damaging the polymer surface.
[14] G. Bar, Y. Thomman, R. Brandsch, H.J. Cantow, M.H. Whangbo, Langmuir 13 (1997) 3807.
[15] S.N. Magonov, V. Elings, W.H. Whangbo, Surf. Sci. Lett. 375 (1997) 385.
[16] N.A. Burnham, O.P. Behrend, F. Oulevey, G. Gremaud, P.-J. Gallo, D. Gourdon, E. Dupas, A.J. Kulik, H.M. Pollock, G.A.D. Briggs, Nanotechnology 8 (1997) 67.
[17] S. Coppée, V.M. Geskin, R. Lazzaroni, P. Damman, Macromolecules 37 (2004) 244.
[18] J. Gierschner, M. Ehni, H.-J. Egelhaaf, B. Miliàn Medina, D. Beljonne, H. Benmansour, G.C. Bazan, J. Chem. Phys. 123 (2005) 144914.
[19] A. Zen, M. Saphiannikova, D. Neher, J. Grenzer, S. Grigorian, U. Pietsch, U. Asawapirom, S. Janietz, U. Scherf, I. Lieberwirth, G. Wegner, Macromolecules 39 (2006) 2162.
[20] A. Facchetti, M.-H. Yoon, T.J. Marks, Adv. Mater. 17 (2005) 1705.
[21] Thinner dielectrics could have been employed in order to increase the gate-induced electric field. For reproducible electrical characteristics, we avoided on purpose very thin dielectrics that might be stressed by the nanorubbing process.
[22] M.L. Chabinyc, J.P. Lu, R.A. Street, Y. Wu, P. Liu, B.S. Ong, J. Appl. Phys. 96 (2004) 2063.
[23] J.N. Haddock, X. Zhang, S. Zheng, Q. Zhang, S.R. Marder, B. Kippelen, Org. Electron. 7 (2006) 45.
[24] Z. Bao, A. Dodabalapur, A.J. Lovinger, J. Appl. Phys. Lett. 69 (1996) 4108.
[25] H. Sirringhaus, N. Tessler, D.S. Thomas, P.J. Brown, R.H. Friend, Adv. Solid-State 39 (1999) 101.
[26] A.R. Brown, C.P. Jarrett, D.M. de Leeuw, M. Matters, Synth. Met. 88 (1997) 37.
[27] J. Veres, S. Ogier, G. Lloyd, D.M. de Leeuw, Chem. Mater. 16 (2004) 4543.
[28] J. Rhayem, M. Valenza, D. Rigaud, N. Szydlo, H. Lebrun, J. Appl. Phys. 83 (1998) 3660.
[29] B.H. Hamadani, D. Natelson, Appl. Phys. Lett. 84 (2004) 443.
[30] E.J. Meijer, G.H. Gelinck, E. van Veenendaal, B.-H. Huisman, D.M. de Leeuw, T.M. Klapwijk, Appl. Phys. Lett. 82 (2003) 4576.
[31] Z. Hu, B. Muls, L. Gence, D.A. Serban, J. Hofkens, S. Melinte, B. Nysten, S. Demoustier-Champagne, A.M. Jonas, Nano Lett. 7 (2007) 3639.